1   **Engineering an Au Nanostar-based Liquid Phase Interfacial**

2   **Ratiometric SERS platform with Programmable Entropy-driven**

3   **DNA Circuits to Detect Protein biomarkers in clinical samples**

4   **Guanli Fan,[a] Xiaorong Gao,[a] Shuling Xu,[a] Xia Li,[a] Qi Zhang,[a] Caifeng Dai,[b*]**

5   **Qingwang Xue,[a*] Huaisheng Wang[a]**

6   [a] *Department of Chemistry, Liaocheng University, Liaocheng, 252059, Shandong,*

7   *China*

8   [b]*Center for Reproductive Medicine, Department of Obstetrics and Gynecology, Qilu*

9   *Hospital of Shandong University, Ji'nan 250012, Shandong, P.R. China*

10

11

12

13

14

15

16

17

18

19

20

21

22   *Corresponding author:

23   Tel: +86-635-8239001; Fax: +86-635-8239001

24   Email: xueqingwang1983@163.com; daicaifeng1982@163.com

25

26

27 **Experimental section.**

28 **Chemicals and Instrumentations.**

1   Streptavidin magnetic nanosphere (SA-MNS, 350 nm in diameter) were
2 purchased from Bangs Laboratories Inc. (Fishers, IN). Mucin 1(MUC1) ELISA Kit
3 was obtained from North Connaught Biotechnology Co. Ltd. (Shanghai, China). DNA
4 oligonucleotides (**Table S1**) were synthesized and HPLC-purified by Sangon
5 Biological Engineering Technology & Services Co., Ltd. (Shanghai, China). HAuCl$_4$
6 was purchased from Shanghai Civic Chemical Technology Co., Ltd. (Shanghai,
7 China). C$_6$H$_5$Na$_3$O$_7$•2H$_2$O was purchased from Tianjin Fengchuan Chemical Reagent
8 Technology Co., Ltd. (Tianjin, China). Ethanol was purchased from Tianjin Fuyu
9 Fine Chemical Co., Ltd. (Tianjin, China). Hexane was purchased from Tianjin
10 Komiou Chemical Reagent Co., Ltd. (Tianjin, China). The other reagents used were
11 analytical grade and can be used directly without further purification. Ultrapure water
12 (Milli-Q, Millipore, resistance 18.2 MΩ cm) was used to prepare all solutions.

Table S1. Sequences of Oligonucleotides Used in the Study

Name		Sequence (5′−3′)
mucin aptamer	1	GCAGTTGATCCTTTGGATACCCTGG
P1DNA		GTCCAAAGGATCAACTGCAGCA
DNA1		TGCTGCAGTTGATCCTTTGGACAGGGCCGTAAGTTAGT TGGAGACGTAGGTTTTTTTTTTTTTTTTTTTT-Biotin
DNA2		ROX-CCACATACATCATATTCCCTGTCCAAAGGATCA ACT
DNA3		CCTACGTCTCCAACTAACTTACGG
F-DNA		CCTACGTCTCCAACTAACTTACGGCCCTGTCCAAAGGA TCAACT-MB

13

14 **Instrumentation.** The spectra of UV−vis absorption was measured on a UH-4150
15 UV-Vis spectrometer, Transmission electron microscopy (TEM) was performed using
16 a JEM-2100 (JEOL, Japan). The morphology features of materials and oil-water
17 interface were observed by ascanning electron microscope (SEM, Hitachi, Japan).
18 Surface-enhanced Raman scattering spectrometer were conducted using a Renishaw
19 InVia Reflex confocal microscope equipped with a 50× objective and a high-

1 resolution grating with 1800 grooves per centimeter. SERS spectra were acquired of

2 633 nm as the excitation wavelength with an exposure time of 1 s.

Self-Assembled Au Nanostars (Au NSs) on Liquid-Liquid Interface

4 The multangular Au nanostars (Au NSs) were prepared through a seed-mediated

5 growth method. [1,2] Briefly, 300 μL of aqueous 10 μM HAuCl$_4$ were first injected into

6 30 mL boiling deionized water under vigorous stirring, next, 100 mL of 40 mM

7 sodium citrate was added. The solution was finally cooled slowly to room temperature

8 under stirring with 700 rpm until the color of the gold colloidal sol turns burgundy to

9 get the Au seed solution.

10 The Au NSs were synthesized by seed-mediated growth. First, ∼10 nm Au seeds

11 were synthesized through a modified turkevich method. Then, 25 μL of aqueous 100

12 mM HAuCl$_4$ was put into 10 mL of deionized water under vigorous stirring.

13 Subsequently, 50 μL of gold seeds, 22 μL of 1% sodiumcitrate, and 1000 μL of 30

14 mM hydroquinone were added one by one. Finally, the solution was kept under

15 stirring at room temperature for 30 minutes to obtain AuNSs.

16 The self-assembled multangular Au NSs at the hexane-water interface was

17 obtained. Briefly, 1.0 mL Au NSs and 1.3 mL hexane were added into a centrifuge

18 tube. Then, ethyl alcohol, which was responsible for the inducer of the self-assembly

19 on the immiscible interface, was injected constantly below the interface. Finally,

20 inerratic Au NSs on the liquid-liquid interface were obtained with continuous shaking.

Preparation of multi-chain composite structure DNA probe

22 5 μL of 1 μM DNA1, 5 μL of 1 μM DNA2, and 5 μL of 1 μM DNA3 were first

23 added to 20 μL of 10 mM PBS buffer (pH = 7.4), and reacted for 30 min at room

24 temperature to form an DNA3-DNA1-DNA2 dsDNA, a three-chain composite

25 structure DNA probe. Subsequently, 20 μL (1 mg mL^{-1}) of streptavidin magnetic

26 nanosphere (MNS) were washed three times to remove surfactants with 200 μL of

27 PBS-T buffer (pH 7.4), and were added to the above-mentioned three-chain

28 composite structure DNA probe solution and reacted for 60 min. Then, the resultant

29 MNS-DNA3-DNA1-DNA2 composite magnetic probe were rinsed with PBS-T and

PBS, respectively, three times. Finally, the magnetic probe was resuspended in 35 μL of PBS buffer, and stored at 4 °C.

Procedure of mucin 1 analysis by the ratiometric SERS strategy based on Entropy-driven DNA Circuits-Cooperated Liquid−Liquid Self-Assembled Au Nanostars Interface

First, 5 μL of 15 μM P1DNA and 5 μL of 10 μM aptamer were added to 10 μL of 10 mM PBS buffer, reacted for 30 min at room temperature to form P1-aptamer double-stranded DNA (dsDNA). Then, 5 μL of different concentrations mucin 1 protein were added to the above solution and incubated for 30 min at room temperature, to finish the competition reaction and release free P1DNA. Subsequently, 5 μL composite magnetic probe and 5 μL of 1.0 μM MB-labeled fuel-DNA(F-DNA) were added to the above solution and incubated at 37 ºC for 3 h, to finish the entropy-driven DNA circuits amplification reaction and release free ROX-labeled DNA2. Finally, the resultant supernate was separated and added into the self-assembled mult-angular Au NSs at the hexane-water interface, and the Raman signals were absorbed along with Au NSs on the immiscible interface to finish the SERS measurement using a 633 nm laser excitation by a Renishaw InVia Raman microscope. The Raman signal ratio of I_{ROX}/I_{MB} is proportional to the mucin 1 concentration.

Preliminary Analysis of Real Sample

Healthy human serum was filtered with 100 kDa ultrafiltration membranes at 10000 rpm 10 min to remove the ions and macromolecules. The ultrafiltrates were spiked with Mucin 1 (1.0 fg/mL, 10 fg/mL, 100 fg/mL, 1 pg/mL, and 10 pg/mL final concentration). The following procedures were the same as those describe above in buffer solution.

3. Results and discussion

Assessment of Entropy-Driven DNA Circuit System
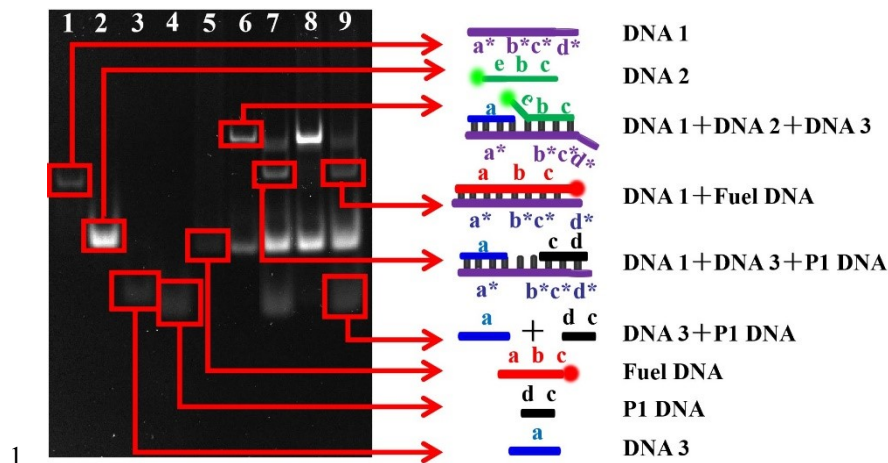
Fig. S1 Native PAGE characterization of different samples in the entropy-driven DNA circuit system. Lane M, 300 bp marker; **Lane 1**, 2.5 μM DNA1; **Lane 2**, 5.0 μM DNA2; **Lane 3**, 2.5 μM DNA3; **Lane 4**, 2.5 μM P1DNA(mimic target); **Lane 5**, 2.5 μM F-DNA; **Lane 6**, 2.5 μM DNA1 + 2.5 μM DNA2 + 2.5 μM DNA3; **Lane 7**, 2.5 μM DNA1 + 2.5 μM DNA2 + 2.5 μM DNA3 + 1.0 μM P1DNA; **Lane 8**, 2.5 μM DNA1 + 2.5 μM DNA2 + 2.5 μM DNA3 + 5.0 μM F-DNA; **Lane 9**, 2.5 μM DNA1 + 2.5 μM DNA2 + 2.5 μM DNA3 + 1.0 μM P1 DNA + 5.0 μM F-DNA.

In the Ratiometric SERS platform, the entropy-driven DNA circuits plays a key role for signal transmit and amplification. Native polyacrylamide gel electrophoresis (PAGE) were performed to investigate the process of entropy-driven DNA circuit. As shown in Fig. S1, the purified DNA1, DNA2, DNA3, P1DNA (mimic target), F-DNA show the bands in lanes **1-5**, respectively. After the reaction of the same concentration of DNA1, DNA2, and DNA3, a bright band with slow migration appeared (lane **6**) than the incubating single strand DNA (lanes **1-3**), indicating the formation of a high molecular weight product of three-chain structured DNA substrate. In the presence of mimic target P1-DNA, lane **7** show additional bands compared with lane **6**, indicating that part of the three-chain structured DNA substrate DNA1-DNA2-DNA3 was converted to byproduct DNA1-DNA3-P1DNA and DNA2 according to the ratiocination of base count. The three-chain structured DNA substrate was stable when Fuel-DNA was introduced (lane **8**), and FDNA and DNA2 cannot be separated due to their nuance of DNA bases. Meanwhile, we observed that the intensity of same concentration DNA 3-DNA 1-DNA 2 dsDNA are not same in Lane **6** and Lane **8**. The

cause of this phenomenon may be attributed to the loss of sample injection quantity when the sample is added to the sample tank in gel electrophoresis experiment. Although there is a difference bright difference in Lane **6** and Lane **8**, the bright difference in Lane **6** and Lane **8** does not affect the gel electrophoresis experimental result that the three-chain structured DNA substrate was stable when Fuel-DNA was introduced. Moreover, compared with lane **7**, P1-DNA and DNA3 were released when the F-DNA was added, and the intermediate DNA1-DNA3-P1DNA was converted to byproduct DNA1-FDNA. It can be seen that the bands of the DNA1-F-DNA and DNA1-P1DNA-DNA3 cannot be separated due to their similar amount of DNA bases (lane **9**). Also, P1DNA cannot be observed due to the trigger of next entropy-driven signal amplification process. The result verified that the entropy-driven DNA circuit based on three-chain-structured DNA substrate was successfully performed.

Characterization of AuNSs and liquid-liquid Self-Assembled Au Nanostars interface

(A)

(B)
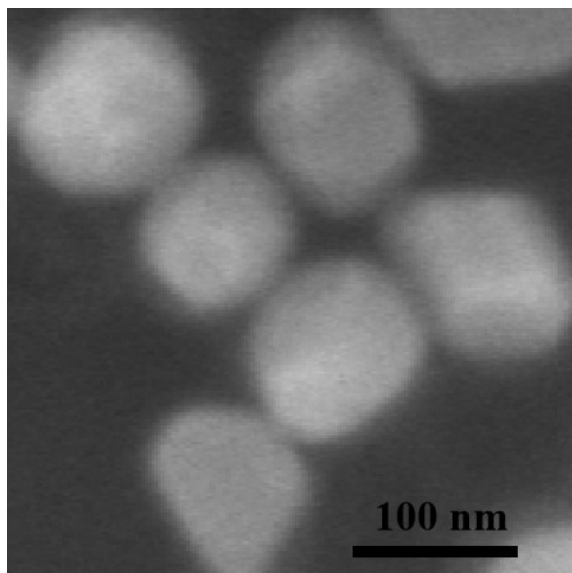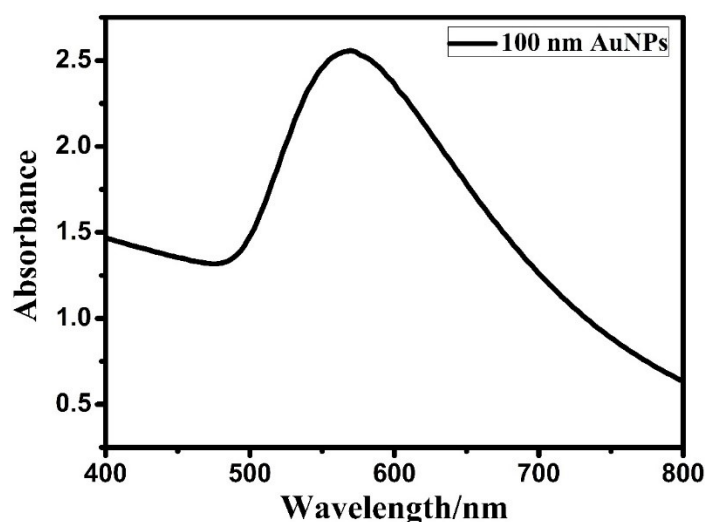
Fig. S2 (A) SEM images of AuNPs. (B) UV-vis absorption spectrum of AuNPs.

Detection Conditions Optimization

In this study, the concentration of aptamer-P1 DNA dsDNA probe caused great effect on the product P1-DNA mimic target as initiator for DNA circuits amplification. Thus, the optimum concentration of aptamer-P1DNA dsDNA detection probe was investigated under 10 pg mL $^{-1}$ target MUC1. **Fig. S3A** revealed the I_{ROX}/I_{MB} signals corresponding to different concentration of aptamer-P1DNA detection probe. The I_{ROX}/I_{MB} signal increase dgradually between 0.5 and 10 μM and reached a relatively stable value at 10 μM. Therefore, 10 μM was selected as the optimum reaction concentration of aptamer-P1DNA dsDNA probe to accelerate the DNA circuits and improve the sensitivity of the proposed biosensor.

In the ratiometric SERS strategy, the I_{ROX}/I_{MB} Raman signal responses were dependent upon the amount of the freed ROX-modified DNA2, and the MB-modified F-DNA bound to magnetic bead. The greater the number of freed ROX-modified DNA2 present, the greater the amount of MB-modified F-DNA bound to magnetic bead. So, a DNA circuits reaction time was expected to yield enhanced I_{ROX}/I_{MB} Raman signal. **Fig. S3**B depicts the effect of entropy-driven DNA circuit reaction time on the I_{ROX}/I_{MB} Raman signal. One observed that the I_{ROX}/I_{MB} increased rapidly with the DNA circuit reaction time up to 2 h and became saturated over 2 h due to the

7

1 exhaustion of signal probe. Thus, 2 h was selected as the optimum time for the

2 entropy-driven DNA circuit reaction.

3   Beyond that, the concentration of MB-modified fuel-DNA affects the DNA

4 circuit reaction and further had great effect on the I_{ROX}/I_{MB} Raman signal. Under low

5 concentration conditions, the DNA circuit reaction could not achieve adequate

6 performance, resulting in a decrease in the release of ROX-modified DNA2 from

7 magnetic bead. On the contrary, high concentration would increase the amount of

8 MB-modified fuel-DNA unbound to magnetic bead, resulting in a high background

9 signal of I_{MB} in separate solution. To investigate the influence of fuel-DNA

10 concentration, a concentration range from 0.1 to 2.5 μM was used for entropy-driven

11 DNA circuit reaction. **Fig. S3**C showed that a peak value of I_{ROX}/I_{MB} appeared at 1.0

12 μM. Therefore, 1.0 μM was chosen as the optimum concentration of Fuel-DNA.

13   Moreover, the parameter of Au NSs volume affecting the SERS platform was

14 also investigated in **Fig. S3**D. When no target exists, with the increasing volume of

15 Au NSs, I_{ROX} remains in a low value due to the trace absorption in the liquid−liquid

16 interface and the I_{MB} enhances because of the different enhancement factor of the

17 substrate. Therefore, the I_{ROX}/I_{MB} decreases until the volume of Au NSs is 1.0 mL,

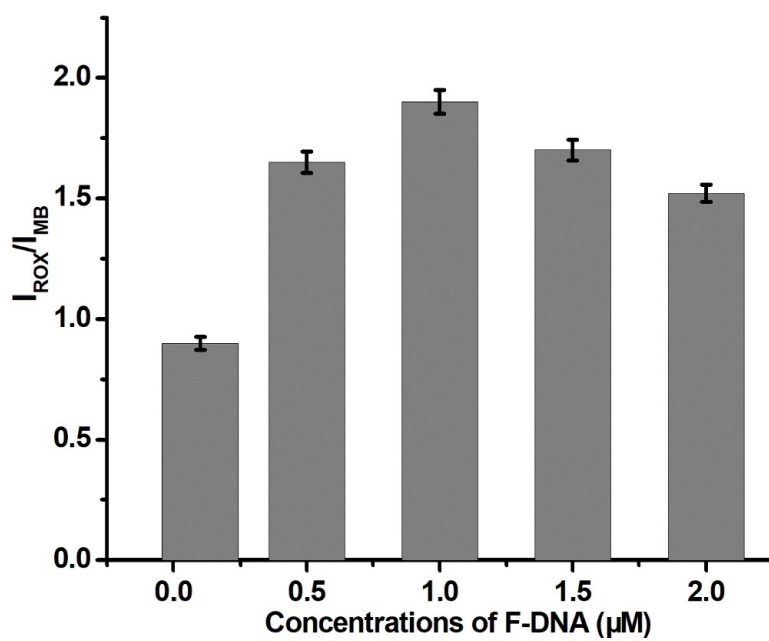18 indicating the optimal state of the liquid−liquid interface.

19

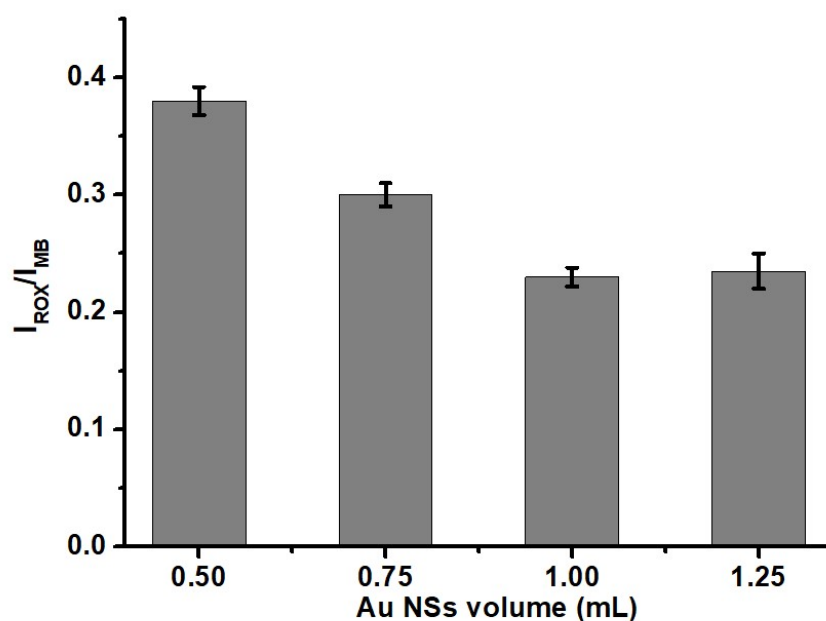20   **(A)**

(B)

1
2
3

(C)

4

5

9

(D)
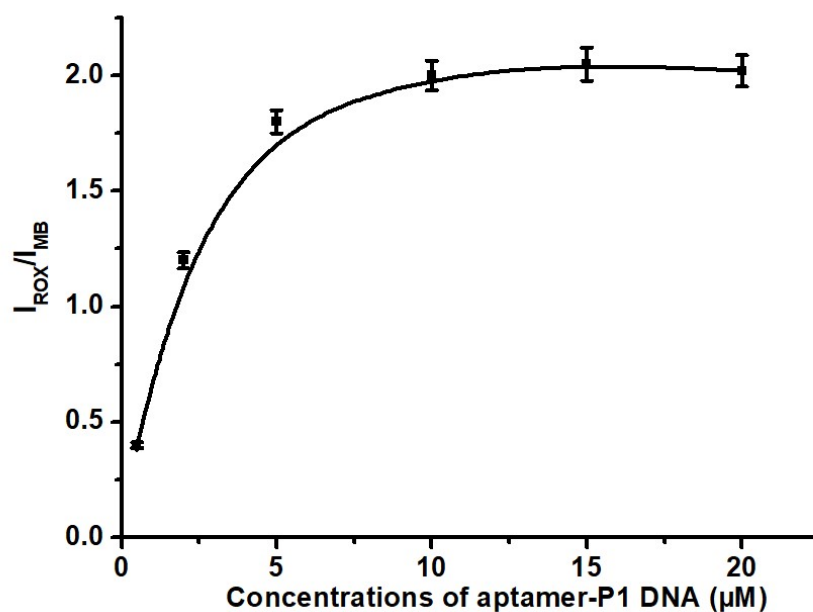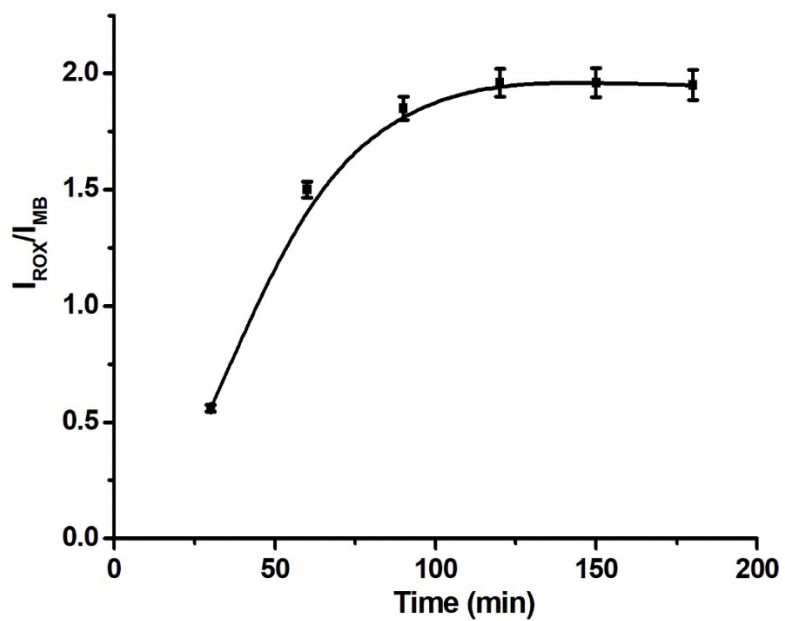
Fig S3. Optimization of (A) aptamer-P1-DNA concentration, (B) entropy-driven DNA circuit reaction time, (C) F-DNA concentration, (D) the volume of Au NSs. The concentration of MUC1 was 10 pg/mL.

**Table S2. Comparison of MUC1 Detection Based on Different Methods**

| Method	System	Linear range	LOD	Reference
FL	RCA-based Immunoassay	0.001-20 ng/mL	0.23 pg/mL	3
ECL	Tetrahedral DNA nanostructure	1.135 fg/ml-0.1135 ng/mL	0.37 fg/mL	4
FL	DNA Tweezer and Fluorescence	0.01-100 pg/mL	2.6 fg/mL	5
FL	CHA and QDs	1 fg/mL-1 pg/mL	0.15 fg/mL	6
ECL	3-D DNA nanomachine	$10^{-3}-10^3$ pg/mL	0.62 fg/ml	7
ECL	T7 Exo-RCA and DNA nanoflowers	$10^{-3}-10^4$ pg/mL	0.23 fg/ml	8
ECL	Tetraphenylethylene microcrystals	1 fg/mL^{-1} -1 ng/mL	0.29 fg/mL	9
SERS 10	Au-Au-UCNP-trimers	0.01-10 fM	0.25 fg/mL	
EC	Nanochannel-sensor	$1-10^4$ fg/mL	0.0364fg/mL	11
SERS	Electrohydrodynamic-Immunoassay	100 pg/mL-10 fg/mL	10 fg/mL	12
ECL	Doped metal-organic nanoplate ECL	10 ng/mL-10 fg/mL	0.14 fg/mL	13
SERS work	DNA circuits and ratiometric	1 fg/mL-10 pg/mL	0.15 fg/mL	this

10

1

2

(A)

3
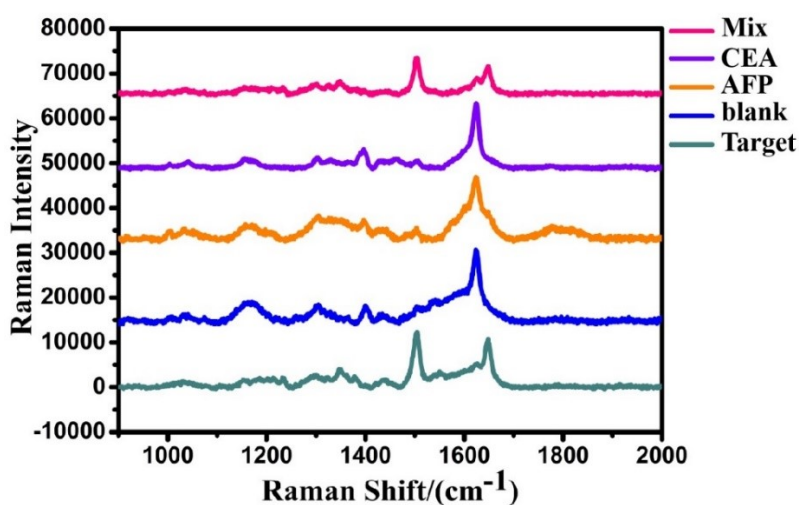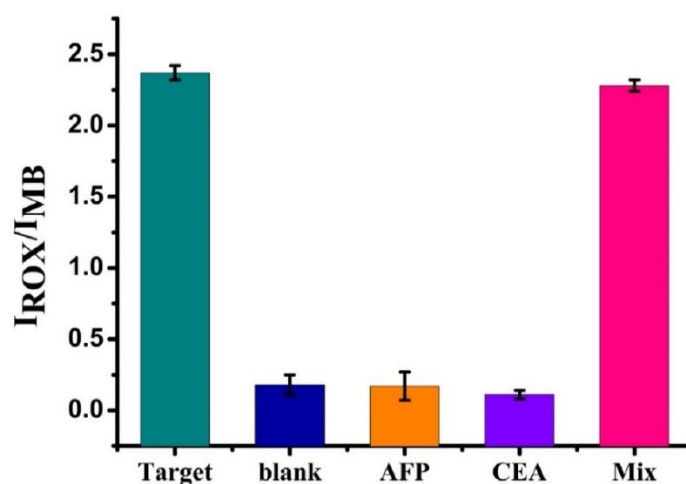
4

5

(B)

6 **Fig. S4** Specificity of the ratiometric SERS sensing platform **(A)** Raman spectra of

7 the SERS platform with differentanalyst (a) 10 pg/mL of MUC1, (b) blank, (c) 10

8 ng/mL of AFP, (d) 10 ng/mL of CEA,(e) a mixture of the samples mentioned above.

9 **(B)** The corresponding Raman I_{ROX} /I_{MB} of the differentanalyst.The error bar

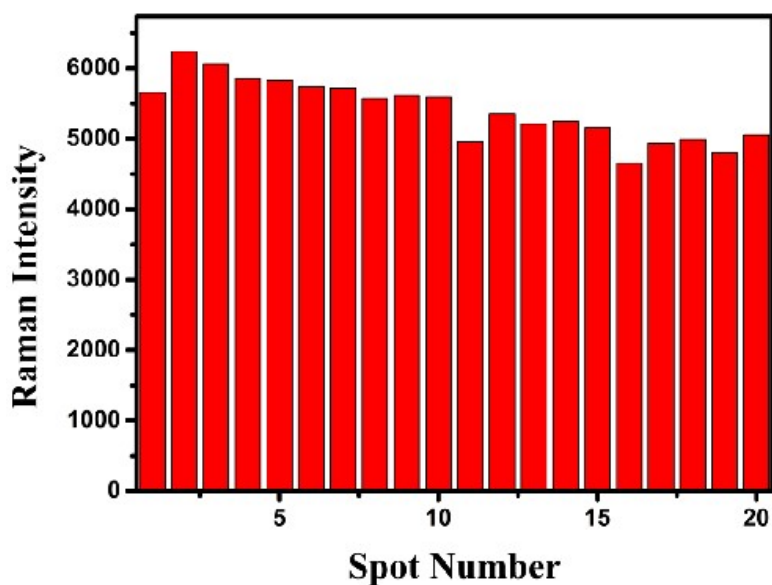10 represents the standard deviation of three measurements.
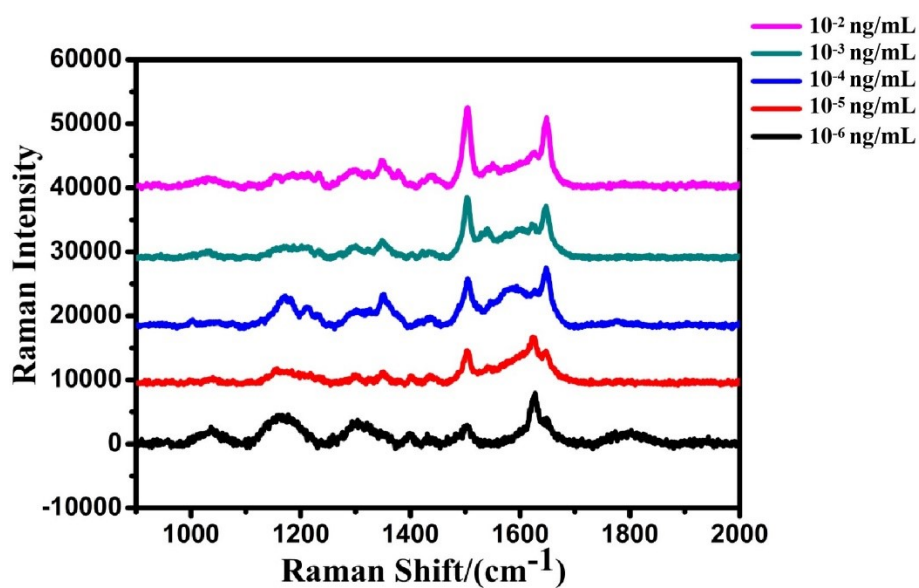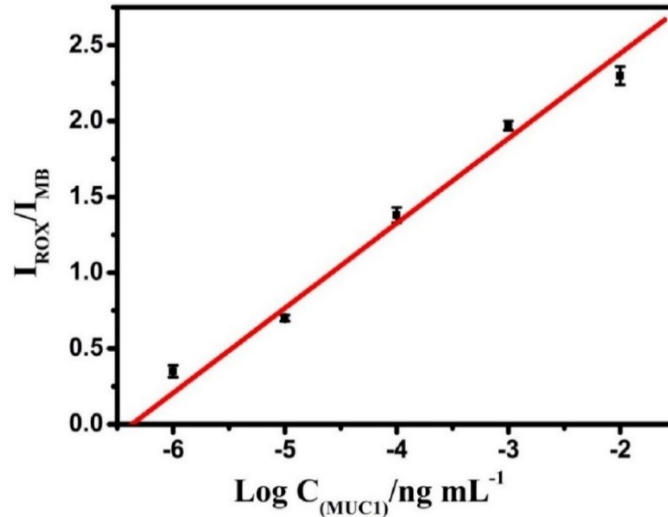
11

1

2
(A)

3

4
(B)

12

(C)

1

2
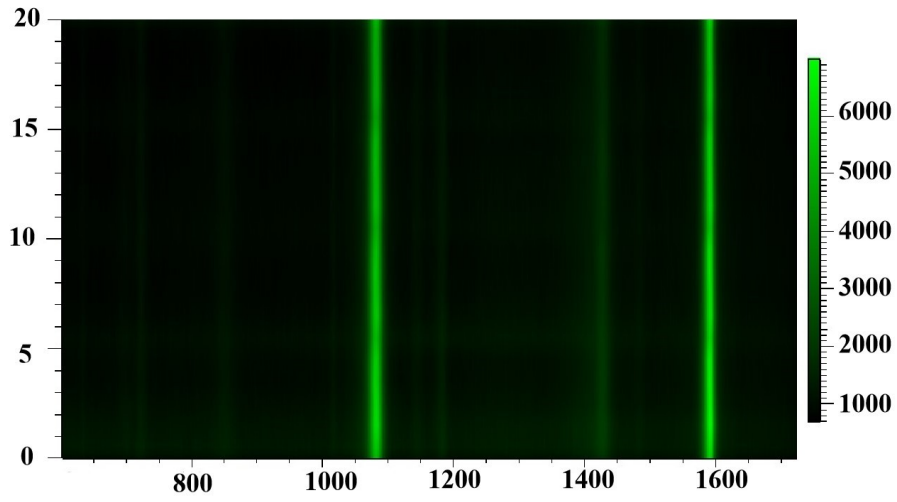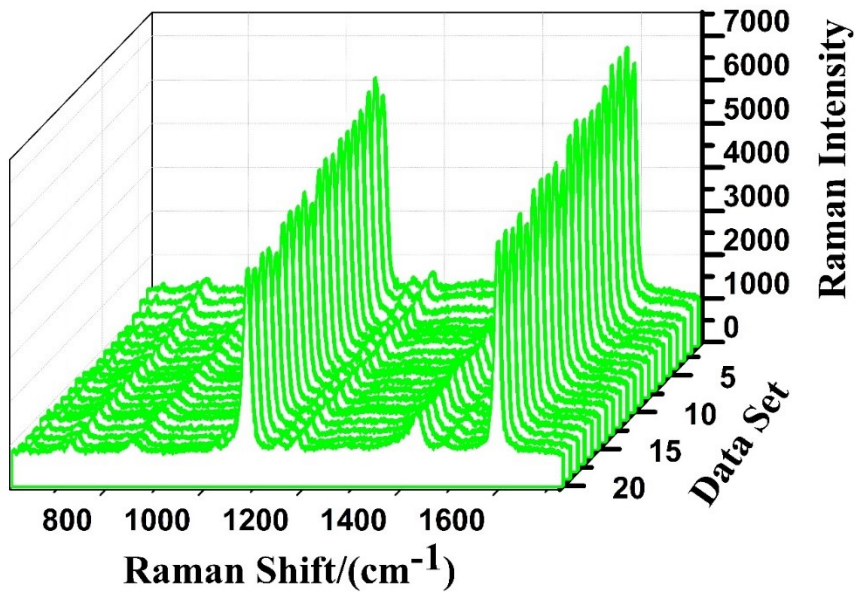
3 **Fig S5. (A)** 20 different spots on the same substrate generating a 2D spectral mapping

4 of 5.0×10^{-7} M 4-MBA. **(B)** Histogram of SERS intensities at 1081 cm^{-1} of the 20

5 spectra. **(C)** the corresponding Raman intensity of the 20 spots.

(A)

6

7

(B)

Fig. S6 Change in the Raman spectra **(A)**, and the ratio value (I_{ROX}/I_{MB})value **(B)** of reaction solution with different concentrations of mucin 1 in human serum. Error bars were estimated from three replicate measurements.

MUC1 Concentration Detection Using a Commercial ELISA Kit

The Mucin 1(MUC1) ELISA Kit assay was carried out according to the instruction. Firstly, a standard curve was performed using standard MUC1 samples at a concentration range from 0.6 to 10 ng/mL. Afterwards, MUC1 concentration of different samples was evaluated by comparison with the standard curve.
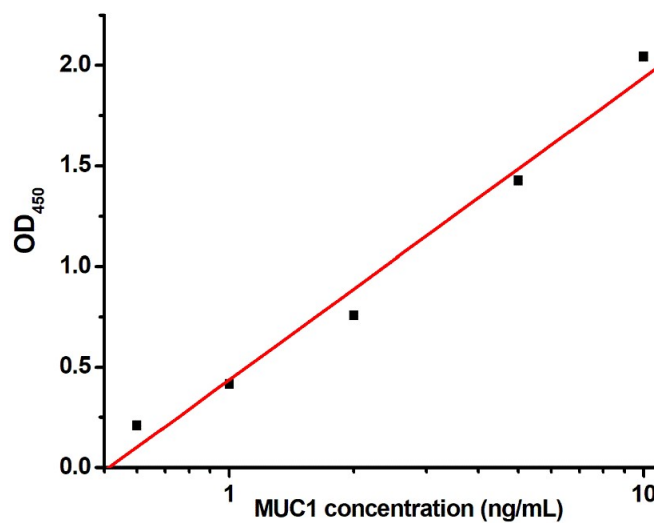
Fig S7. Linear relationship between optical density at 450 nm and standard MUC1 concentration using a Mucin 1(MUC1) ELISA Kit.

14

Table S3. Recovery Results for MUC1 Determination In Human Serum Samples

Spiked (pg/mL)	ELISA(pg/mL)	Recovery (%)	Our strategy(pg/mL)	Recovery (%)
1.00	Not detected	\	0.96±0.04	96
5.00	Not detected	\	5.1±0.02	102
10.00	Not detected	\	10.3±0.5	103

1

2

Table S4 Comparison of real blood sample detection.

Sample	ELISA		Our strategy	
	MUC1(ng/mL)	RSD	MUC1(ng/mL)	RSD
1	9.056	0.035	9.125	0.042
2	8.527	0.04	8.483	0.038
3	8.713	0.032	8.658	0.045
4	9.567	0.05	9.612	0.028

3

4 **REFERENCES**

5 (1) Tanwar, S.; Haldar, K. K.; Sen, T. *J. Am. Chem. Soc.* **2017,** *139* , 17639-17648.

6 (2) Cao, X.; Shi, C.; Lu, W.; Zhao, H.; Wang, M.; Zhang, M.; Chen, X.; Dong, J.;

7 Han, X.; Qian, W. *J. Nanosci. Nanotechnol.* **2016,** *16* , 12161-12171.

8 (3) Yang, W. T.; Shen, Y.; Zhang, D. Y.; Xu, W. J. Chem. Commun. 2018, 54,

9 10195−10198.

10 (4) Wei, Y. P.; Zhang, Y. W.; Mao, C. J. A. J. Mater. Chem. B. 2020, 8, 2471-2475.

11 (5) Yang, W.; Shen, Y.; Zhang, D.; Li, C.; Yuan, R.; Xu, W., Anal Chem. 2019, 91,

12 7782-7789.

13 (6) Chen, P.P.; Wang, Y.; He, Y.Q; Huang, K.; Wang, X.; et al. ACS Nano. 2020, 15,

14 11634–11643.

15 (7) Jiang, X. Y.; Wang, H. J.; Wang, H. J.; Zhuo, Y.; Yuan, R.; Chai, Y. Q. Anal.

16 Chem. 2017, 89, 4280−4286.

17 (8) Li, S. K.; Chen, A. Y.; Niu, X. X.; Liu, Z. T.; Du, M.; Chai, Y. Q.; Yuan, R.; Zhuo,

18 Y. Chem. Commun. 2017, 53, 9624−9627.

19 (9) Jiang, M. H.; Li, S. K.; Zhong, X.; Liang, W. B.; Chai, Y. Q.; Zhuo, Y.; Yuan, R.

20 Anal. Chem. 2019, 91, 3710-3716.

21 (10) Qu, A. H.; Wu, X. L.; Xu, L. G.; Liu, L. Q.; Ma, W.; Kuang, H.; Xu, C. L.

Nanoscale. 2017, 9, 3865-3872.

(11) Pan, M.Y; Cai, J.R; Li, S.; Xu, L.G.; Ma, W.; Xu, C.L,; Kuang, H. Anal. Chem. 2021, 93, 4825–4831.

(12) Kamil Reza, K.; Wang, J.; Vaidyanathan, R.; Dey, S.; Wang, Y.; Trau, M., Small 2017, 13, 1602902.

(13) Yao, L.; Yang, F.; Liang, W.; Hu, G.; Yang, Y.; Huang, W.; Yuan, R.; Xiao, D., Sensor Actuat B-Chem 2019, 292, 105-110.